**Accepted Manuscript**

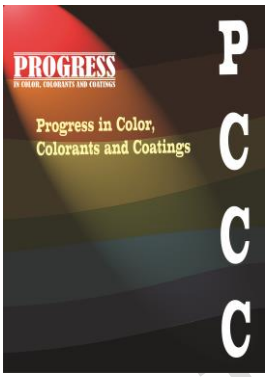


**Title: Comparative Study of Surfactants in Graphene Conductive Inks: From Dispersion Mechanisms to Electrical Properties**

**Authors:** Nazanin Valizadeh, Mojtaba Jalili, Farhad Ameri, Mohsen Mohammad Raei Naeini

Manuscript number**: PCCC-2505-1398**

To appear in: Progresss in Color, Colorants and Coatings

Received: 21 May 20254

Final Revised: 18 August 2025

Accepted: 20 Agugust 2025

Please cite this article as:

N. Valizadeh, M. Jalili, F. Ameri, M. Mohammad Raei Naeini, Comparative Study of Surfactants in Graphene Conductive Inks: From Dispersion Mechanisms to Electrical Properties, Prog. Color, Colorants, Coat., 19 (2026) XX-XXX.

DOI: 10.30509/pccc.2025.167556.1398

# Comparative Study of Surfactants in Graphene Conductive Inks: From Dispersion Mechanisms to Electrical Properties

Nazanin Valizadeh[1], Mojtaba Jalili[1]*, Farhad Ameri[2]*, Mohsen Mohammad Raei Naeini[1]

1. Department of Printing Science and Technology, Institute for Color Science and Technology, P. O. Box: 16765-654, Tehran, Iran.
2. Department of Color Physics, Institute for Color Science and Technology, P. O. Box: 16765-654, Tehran, Iran

* Mojtaba Jalili: jalili@icrc.ac.ir, ** Farhad Ameri, fameri@icrc.ac.ir,



## Abstract

The development of environmentally friendly, water-based conductive inks with exceptional dispersion stability and electrical conductivity is crucial for advancing next-generation printed electronics. This study systematically investigates the effects of surfactant type (SDBS, SDS, CTAB, and Triton X-100) and concentration on the dispersion stability and conductivity of graphene-based conductive inks. After scrutinizing the effect of surfactant type, the influence of its concentration has been investigated by sweeping the surfactants concentration in the range of 0.1% to 0.75% (w/w). Moreover, the effects of surfactant concentration and various milling process (Ultrasonication, Jar Milling, and Magnetic Stirring) on conductivity are studied. UV-Vis. spectrophotometry, turbidimetry, particle size analysis, SEM, Confocal Raman analysis and four probe conductivity- meter are used for evaluation of dispersion stability and conductivity. Results revealed that anionic surfactants, particularly SDBS, outperformed cationic and nonionic surfactants due to enhanced electrostatic repulsion

and π-π interactions with graphene. It was revealed that the optimal properties are obtainable by SDBS with 0.1% (w/w), far below its critical micelle concentration which minimized micelle formation and improved conductivity. Magnetic stirring emerged as the most effective dispersion method, minimizing structural defects and achieving the lowest electrical resistivity (24-32 mΩ). The optimized formulation (0.1% SDBS with magnetic stirring) resulted in a 15% reduction in electrical resistivity compared to the standard formulation. The findings provide a rational framework for surfactant selection and ink formulation, paving the way for high-performance conductive inks in flexible electronics and other applications.

**Keywords:** Conductive ink, Printed electronics, Graphene, Nano particles, Dispersion

## 1. Introduction

The rapid advancement of printed electronics technology has created a growing demand for conductive inks with superior performance characteristics. These specialized formulations serve as essential components in diverse applications ranging from flexible displays and smart packaging to photovoltaics, radio frequency identification (RFID) tags, and wearable electronics [1, 2]. Among the various categories of conductive inks available, water-based formulations have gained significant attention due to their environmental friendliness, cost-effectiveness, reduced toxicity, and processing advantages compared to solvent-based alternatives that often contain volatile organic compounds [3, 4].

Water-based conductive inks offer several distinct advantages, including compatibility

with a wide range of substrates, reduced environmental impact, and enhanced workplace safety. However, these benefits come with inherent challenges related to formulation stability and performance optimization [5-7]. A critical challenge in the development of water-based conductive inks is achieving and maintaining dispersion stability. Conductive particles in aqueous media—whether metallic (e.g., silver, copper), carbon-based (e.g., graphene, carbon nanotubes), or composites—tend to agglomerate due to strong van der Waals forces, hydrophobic interactions, and high surface energy, resulting in sedimentation and plummet in electrical conductivity [8, 9].

This instability presents a significant barrier to large-scale industrial adoption, as it affects both shelf life and printing consistency. Particle agglomeration can lead to nozzle clogging in inkjet printing systems, uneven film formation in screen printing, and ultimately inconsistent conductivity in the printed patterns [10]. Consequently, developing methodologies to enhance dispersion stability represents a crucial research direction in the field of printed electronics.

Surfactants play a pivotal role in stabilizing particle dispersions by modifying interfacial properties between the conductive particles and the aqueous medium [11-13]. These amphiphilic molecules can provide electrostatic repulsion, steric hindrance, or a combination of both mechanisms (electrosteric stabilization) to prevent particle aggregation. Electrostatic stabilization occurs when charged surfactant molecules adsorb onto particle surfaces, creating a repulsive force between similarly charged particles. Steric stabilization results from the physical barrier created by bulky surfactant molecules or polymers adsorbed on particle surfaces, preventing close approach and agglomeration [14, 15].

The selection of appropriate surfactants is critical for optimizing ink formulations, as these additives influence not only dispersion stability but also viscosity, surface tension, substrate wetting, and ultimately the electrical performance of printed features [16]. Different classes of surfactants e. g. anionic, cationic, nonionic, and zwitterionic offer distinct advantages and limitations based on their molecular structure and interaction mechanisms with specific types of conductive particles and substrates [17-19].

Despite their recognized importance, a comprehensive understanding of how different surfactant types affect dispersion stability at varying concentrations remains inadequately explored in the context of water-based conductive inks. While the general principles of colloidal stabilization are well-established, their specific application to conductive materials in printing formulations presents unique challenges that require systematic investigation [20, 21]. The critical micelle concentration (CMC), beyond which surfactant molecules form micelles in solution rather than adsorbing to particle surfaces, represents an important parameter that varies significantly among surfactant types and can dramatically influence dispersion behavior [22].

Previous studies have primarily focused on individual surfactant types or narrow concentration ranges, often without a comprehensive comparative analysis of different stabilization mechanisms. For example, in a prominent study [23], the effectiveness of various surfactants for nanoparticle dispersion has been investigated but conductive ink applications did not specifically target. Chen and co-workers [24] explored the effects of surfactant concentration on graphene dispersions, though their investigation was limited to a narrow selection of surfactants. Similarly, Ref. [24] examined the role of anionic surfactants in stabilizing silver nanoparticle inks, yet failed to provide a comparative

analysis with cationic or nonionic alternatives. This fragmented body of research has resulted in a knowledge gap concerning the relative effectiveness of different surfactant classes and their optimal concentration ranges for conductive ink formulations.

Furthermore, a critical shortcoming in the existing literature is the lack of attention to how surfactant concentration—particularly in relation to its critical micelle concentration (CMC)—influences the electrical conductivity of final printed inks. Another underexplored factor is the impact of dispersion methods: while effective dispersion requires sufficient shear to exfoliate and stabilize graphene sheets, excessive mechanical treatment may compromise the structural integrity of the nanosheets, thereby diminishing conductivity. Thus, a key open question remains: Which dispersion method strikes the best balance between effective dispersion and minimal structural damage to graphene?

The present study addresses these gaps by systematically examining the effects of surfactant type, concentration (relative to CMC), and dispersion method on the stability and electrical performance of water-based graphene inks. Representative surfactants from each major class were selected: sodium dodecyl benzene sulfonate (SDBS) and sodium dodecyl sulfate (SDS) as anionic surfactants; cetyltrimethylammonium bromide (CTAB) as a cationic surfactant; and Triton X-100 as a nonionic surfactant. The influence of surfactant concentration was investigated as well to identify the optimal concentration regarding to the surfactant's CMC. The influence of dispersion technique—ultrasonication, jar milling, and magnetic stirring—was also investigated, offering a comprehensive evaluation of factors affecting printable graphene ink performance.

## 2. Experimental

### 2.1. Materials

All surfactants (SDBS, SDS, CTAB, and Triton X-100) were purchased from Merck with >99% purity. Graphene nanoplatelets (Grade M, average thickness: 6-8 nm, average lateral size: 5 μm) were obtained from XG Sciences Inc. Deionized water (resistivity > 18.2 MΩ·cm) was used for all experiments.

### 2.2. Sample preparation

While the primary objective of this study was not to develop a commercially viable conductive ink, the focus was on optimizing the dispersion stability and electrical conductivity of aqueous graphene suspensions while preserving the nanosheets' planar structure. As such, the ink formulations were intentionally simplified by including only essential components—namely, graphene and surfactants—and omitting additional ingredients such as binders, viscosity modifiers, or humectants. This approach helped minimize confounding variables and allowed for a more systematic analysis of the effects of surfactant type, concentration, and dispersion method. Despite their simplified composition, the resulting graphene dispersions are compatible with multiple printing technologies, including flexographic and gravure printing.

### 2.3. Investigating the effect of surfactant type

Four different surfactants were used under identical laboratory conditions at 25 °C and pH 7.0 to create stable graphene dispersions. At this stage, four separate aqueous surfactant solutions were prepared, each containing 0.25% (w/w) of one of the following surfactants: SDBS, SDS, Triton X-100, and CTAB. To ensure complete dissolution of the

surfactants, each solution was stirred using a magnetic stirrer at 500 rpm for 60 minutes at ambient temperature. Subsequently, 0.75% (w/w) graphene was added to each solution, and stirring was continued for an additional 60 minutes.

Following the evaluation of different surfactants, the effect of dispersion method on both dispersion quality and electrical performance of the inks was investigated. Graphene inks were prepared using three different dispersion techniques: a jar mill, an ultrasonic device, and a magnetic stirrer. The mechanisms responsible for dispersion and particle size reduction vary across these systems. For this comparison, three samples were prepared—each containing 0.75% (w/w) graphene and 0.25% (w/w) SDBS surfactant, as previously described. The only variable was the dispersion method.

Ultrasonic treatment was conducted using an ultrasonic device operated at 70% intensity for 90 minutes, with a pulse interval of 0.5 seconds. Jar mill dispersion was performed by placing 25 g of the dispersion mixture into a milling vessel along with 190 g of zirconia grinding media (0.8–1 mm diameter), followed by milling at 175 rpm for 120 hours. Magnetic stirring was conducted by gently agitating 25 g of the mixture in a 50 mL beaker using a 20 mm magnetic bar at 500 rpm for 24 hours.

After identifying the most effective surfactant and dispersion method, the effect of surfactant concentration was studied. Surfactant concentrations were selected to evaluate dispersion stability below, near, and above the critical micelle concentration (CMC) of the chosen surfactant (SDBS). The initial concentration of 0.25 wt% for each surfactant was selected based on values reported in prior studies [15, 18]. Given that the CMC of SDBS in aqueous solution is approximately 0.2% (w/w) [25], the initial amount was slightly above its CMC. To further investigate the effect of surfactant concentration

relative to its CMC on dispersion quality, two additional concentrations (0.1 wt% and 0.75 wt%) were tested in the case of SDBS.

Table 1: Summary of graphene ink formulations and preparation methods

| Sample name | Component's concentration (w%) | | | Dispersant | Dispersion technique |
|---|---|---|---|---|---|
| | Graphene | Dispersant | Water | | |
| SDBS-0.25-US | 0.75 | 0.25 | 99 | SDBS | Ultrasonic |
| SDS-0.25-US | 0.75 | 0.25 | 99 | SDS | Ultrasonic |
| CTAB-0.25-US | 0.75 | 0.25 | 99 | CTAB | Ultrasonic |
| TX100-0.25-US | 0.75 | 0.25 | 99 | Triton X-100 | Ultrasonic |
| SDBS-0.25-JM | 0.75 | 0.25 | 99 | SDBS | Jar mill |
| SDBS-0.75-MS | 0.75 | 0.75 | 98.5 | SDBS | Stirring |
| SDBS-0.25-MS | 0.75 | 0.25 | 99 | SDBS | Stirring |
| SDBS-0.10-MS | 0.75 | 0.1 | 99.15 | SDBS | Stirring |



### 2.4. Characterization

**Morphological Analysis:** Graphene morphology was examined using a Field Emission Scanning Electron Microscope (FE-SEM, TESCAN MIRA III) operated at an accelerating voltage of 10 kV. Samples were prepared by drop-casting appropriately diluted dispersions onto clean silicon wafers, followed by air-drying at room temperature. Prior to imaging, all samples were coated with a thin gold layer using an electro-sputtering system to improve conductivity and prevent charging.

**Structural Analysis:** Raman spectroscopy was performed using a Horiba Xplora PLUS

system equipped with a 532 nm laser (0.5 mW power) and a Syncerity OE detector. Spectra were collected with a 1 μm spot size and an integration time of 10 seconds. Data analysis and peak fitting were carried out using OriginPro 2016 software to evaluate structural defects in the graphene nanosheets.

**Electrical Characterization:** Electrical conductivity was assessed by measuring sheet resistance using a four-point probe setup (Keithley 2400 SourceMeter). Conductive films were fabricated by drop-casting the ink formulations onto glass substrates, followed by thermal drying at 120°C for 2 hours to ensure complete solvent evaporation and film formation.

**Dispersion Stability Analysis:** The dispersion quality and stability of graphene were assessed using UV–Visible spectroscopy (Shimadzu UV-1800) over the wavelength range of 200–800 nm. Prior to measurement, each sample was diluted 1:100 with deionized water to ensure the absorbance remained within the spectrophotometer's linear response range. In this analysis, graphene is treated as a light-absorbing species, where better-dispersed graphene nanosheets are expected to exhibit stronger light absorption due to reduced aggregation and increased effective surface area. Consequently, lower transmittance (or higher absorbance) in the UV–vis spectrum can qualitatively reflect a more stable and homogeneous dispersion. This approach provides a comparative insight into the relative dispersion states across different formulations.

## 3. Results and Discussion

### 3.1. The structure of surfactants

In electrically conductive inks based on graphene, the size of graphene nanoparticles, the extent of structural defects, and the aggregation of layers are critical factors. In addition, the stability of the dispersion of graphene sheets within the ink medium is of paramount importance. Therefore, the formulation of graphene-based conductive inks requires

careful consideration to achieve an optimal point between intrinsic properties and dispersion stability, ultimately resulting in an ink with acceptable conductivity and simultaneously acceptable printability. To this end, the characteristics of the ink were assessed, including the geometric shape of the particles, particle size distribution, the level of defects introduced by various dispersion methods or influenced by the types of materials used in the dispersion process, dispersion stability, and, finally, electrical conductivity.

FE-SEM images were employed to investigate the morphology of the resultant nanoparticles, as shown in **Figure 1**. These images correspond to four surfactants: SDBS, SDS, Tri-X100, and CTAB. The type of surfactant utilized can significantly impact the stability of graphene in an aqueous environment [18]. SDS is an anionic linear aliphatic surfactant, SDBS is an anionic linear alkyl phenyl surfactant, CTAB is a cationic linear aliphatic surfactant, and Tri-X100 is a non-ionic ethoxylated branched alkyl phenol surfactant.

Figure 1 suggests that the dispersion performance of graphene using anionic surfactants, SDS and SDBS, are superior compared to cationic and non-ionic surfactants, leading to less damage to the graphene sheets. While CTAB and Triton X-100 show micelle-induced aggregation, SDS and SDBS clearly show better dispersion performance. According to Figure 1, it can be vividly seen that anionic surfactants perform better than cationic and non-ionic surfactants, as they better maintain the lamellar structure of graphene. The samples that contain SDS and SDBS as surfactant, has larger and more distinctive lamellar structure of the graphene nanosheets. It can be interpreted as the superior performance of these anionic surfactants for dispersing nanographene. Thus, it can be concluded that the charge factor plays a significant role in the stabilization and separation of the sheets. However, the superior performance of SDS and SDBS can be also attributed to their linear structure since the presence of side chains in the molecular structures of CTAB and Triton X-100 likely hinders their effective adsorption onto the surfaces of graphene sheets, leading to performance that cannot match that of linear systems.

The superior performance of SDBS in stabilizing graphene dispersions can be attributed to both its molecular structure and electrostatic interaction mechanisms. SDBS, as an anionic surfactant with a delocalized negative charge on its aromatic ring, provides strong electrostatic repulsion between graphene sheets, effectively preventing restacking and aggregation. In contrast, SDS, although also anionic, lacks the aromatic group that facilitates π–π interactions with the graphitic surface, leading to slightly weaker stabilization. The cationic surfactant CTAB may induce partial destabilization due to charge neutralization effects and possible surfactant aggregation on graphene surfaces. Nonionic surfactants like Triton X-100 depend mainly on steric stabilization, which is often less effective in preventing restacking of nanosheets in aqueous systems. These differences explain the variation in dispersion stability observed in UV-Vis, zeta potential, and particle size measurements.

Among the investigated anionic surfactants, SDBS overpowers SDS in stabilizing graphene nanosheets which can be attributed to π-π stacking and electrostatic repulsion.

In the molecular structure of the SDBS surfactant, both linear aliphatic and aromatic

systems are present, allowing the phenyl ring to overlap with the π-electronic cloud of the graphene nanoparticle through π-π stacking [18]. Additionally, the negatively charged sulfonate group ($SO_3^-$) creates electrostatic repulsion, thereby preventing the exfoliated nanosheets from re-stacking. The benzene ring adjacent to the sulfonate group in SDBS, also acts as an electron-withdrawing moiety, enhancing the delocalization and effective negative charge of the sulfonate headgroup. This results in stronger electrostatic repulsion between surfactant-stabilized graphene sheets compared to SDS, which lacks such an aromatic structure. Consequently, SDBS provides superior colloidal stabilization due to its stronger inter-sheet repulsive forces. SDS surfactant on the other hand, has no phenyl ring; which significantly diminishes its tendency to adsorb on the graphene nanosheets surface in comparison with SDBS. The high concentration of CTAB and Tri-X100, resulting in micelles formed on the surface of graphene, is visible in the images. In fact, the concentration used in the conductive inks for these surfactants exceeded the critical micelle concentration (CMC), resulting in undesirable outcomes.

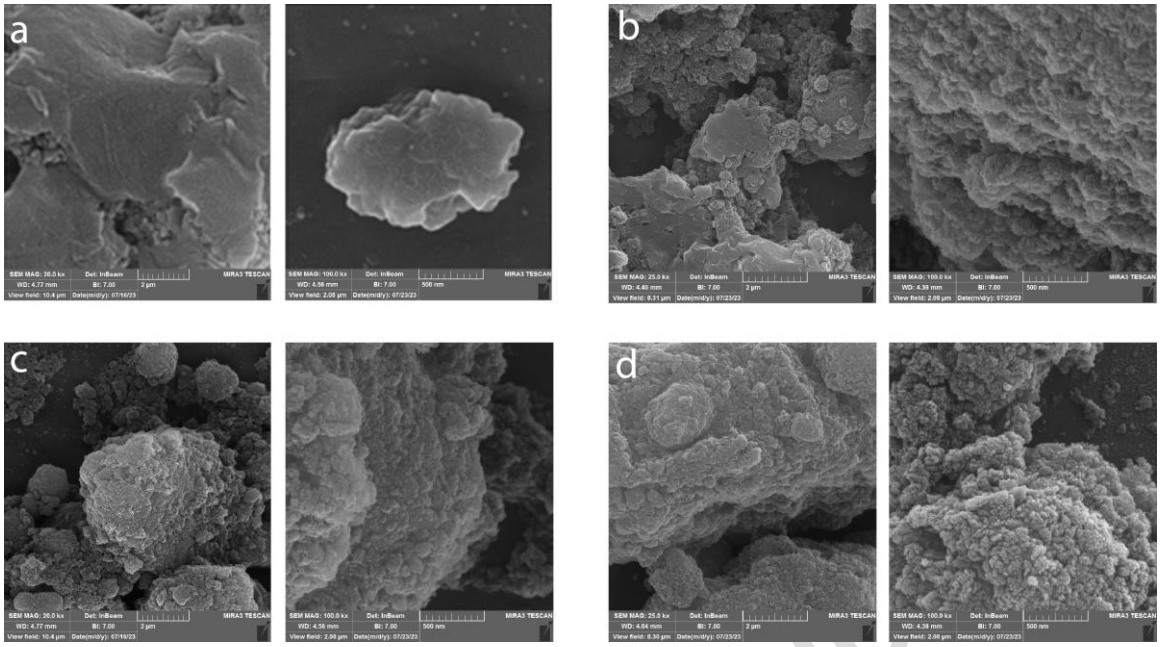


Figure 1: FE-SEM images showing morphological differences of graphene nanoparticles in (a) SDBS-0.25-US, (b) SDS-0.25-US, (c) CTAB-0.25-US, and (d) TX100-0.25-US.

Raman spectroscopy is a powerful tool for identifying structural defects and chemical modifications in graphene. The Raman spectra corresponding to dispersions with each of the four surfactants are shown in Figure 2. The anionic surfactants exhibited similar spectral features, whereas in the cases of cationic and nonionic surfactants, the micelle structures formed on the graphene surface appeared to obscure characteristic Raman peaks, potentially due to surface coverage or scattering interference.

It is well established that graphene exhibits two prominent Raman peaks near 1350 $cm^{-1}$ and 1580 $cm^{-1}$, referred to as the D band and G band, respectively. The D band is attributed to structural defects, edges, and disorder in the $sp^2$ carbon lattice, while the G band arises from the in-plane vibrational modes of $sp^2$-bonded carbon atoms.

The intensity ratio of these bands ($I_D/I_G$) serves as a quantitative indicator of the degree of disorder or damage in the graphene structure. Since the electrical conductivity of graphene nanosheets relies heavily on the π-conjugated network of $sp^2$-hybridized carbon

atoms, preserving this structure during dispersion is critical for applications in printed electronics. Therefore, the $I_D/I_G$ ratio can be used as a criterion to evaluate the effectiveness of different surfactants in dispersing graphene while minimizing structural degradation. The intensity ratio of D band to G band is reported in Table 2. As shown, sample prepared with SDBS has the lowest value, indicating that SDBS dispersed graphene experience the lowest degradation among these four samples.

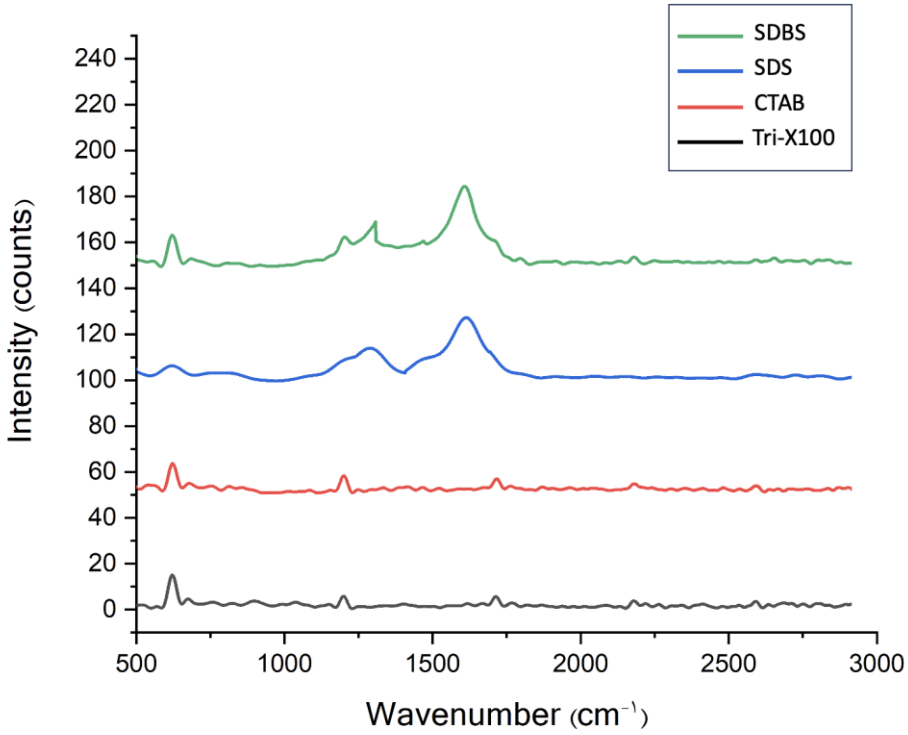


Figure 2: Raman spectra of graphene dispersions with different surfactants

Table 2: Raman spectra data for graphene nano sheets dispersed with various surfactants

| Sample name | G peak position ($cm^{-1}$) | D peak position ($cm^{-1}$) | $\frac{I_D}{I_G}$ |
|---|---|---|---|
| SDBS-0.25-US | 1554 | 1333.1 | $\frac{1}{3}$ |
| SDS-0.25-US | 1593 | 1342 | $\frac{1}{2}$ |

| | | | |
|---|---|---|---|
| TX100-0.25-US | 1672 | 1245.6 | $\frac{3}{1}$ |
| CTAB-0.25-US | 1681 | 1254 | $\frac{2}{1}$ |

Based on the results from FE-SEM imaging and Raman spectroscopy, it was anticipated that graphene dispersed with SDBS would exhibit the lowest electrical resistivity, followed by samples dispersed with SDS. To validate this hypothesis, the electrical resistivity of the corresponding printed films was measured, with the results summarized in Table 3.

As shown, the order of electrical conductivity is in strong agreement with the previous structural characterizations. The SDBS-dispersed sample demonstrated the lowest resistivity, confirming its superior dispersion quality. The SDS-based sample also exhibited conductivity, though to a lesser extent. In contrast, samples containing CTAB and Triton X-100 did not exhibit appreciable electrical conductivity, likely due to poor dispersion or excessive structural damage to the graphene sheets.

These results suggest a direct correlation between the quality of dispersion and the electrical performance of the printed films: better-dispersed graphene leads to improved conductivity, while ineffective dispersion results in poor electrical performance. It aligns well with previously published research that demonstrated the crucial impact of graphene dispersion quality on the electrical properties of related nanocomposites [26, 27].

Table 3: Electrical resistivity of graphene films prepared with different surfactants

| Sample name | Electrical resistivity after heat treatment (MΩ) |
|---|---|
| SDBS-0.25-US | 38-64 |
| SDS-0.25-US | 53-89 |
| TX100-0.25-US | -- |
| CTAB-0.25-US | -- |

UV-Vis. spectroscopy serves as a standard measure for evaluating the dispersion quality of graphene in aqueous solutions. The exact position and shape of absorption bands may vary depending on the molecular structure of each surfactant and its concentration, making this technique a robust and straightforward method for assessing graphene dispersion quality in water. Figure 3 presents the UV-vis spectra of graphene dispersed in water using four different surfactants.

The π-π* transitions of graphene sheets are typically observed in UV-vis spectra, where absorption intensity can be used to analyze the effects of surfactant concentration and dispersion methodology. As depicted in Figure 3, a distinct peak appears near 284 nm in all spectra. This peak corresponds to π-π* transitions of C=C bonds in graphene, which is consistent with previous studies [25].

Among the tested surfactants, SDBS proved most effective in exfoliating graphene sheets and achieving stable aqueous dispersion, as evidenced by its higher absorption intensity. The absorption peak intensity directly correlates with graphene concentration in the colloidal system. Both anionic surfactants demonstrated substantially higher absorption compared to cationic and nonionic surfactants, while the latter two exhibited remarkably similar behavior.

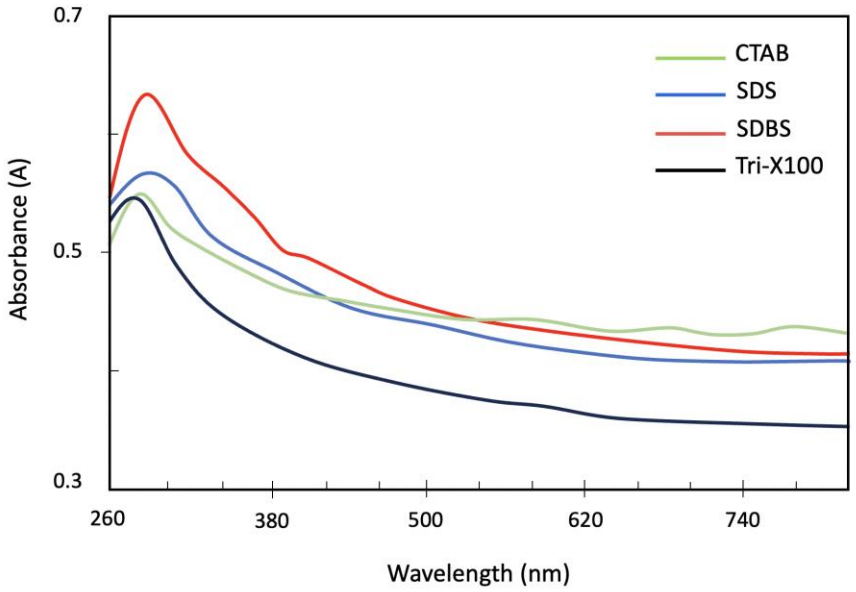


Figure 3**:** UV-vis spectra of graphene dispersions with different surfactants showing the characteristic π-π transition peak at 284 nm

### 3.2. The dispersion method

Given its markedly better performance in the aforementioned experiments, SDBS was selected for extended analysis. In the next phase of the study, the dispersion method (magnetic stirring, ultrasonication, and jar milling) and surfactant concentration (0.1–0.75 wt%) were systematically varied. The aim was to optimize the dispersion protocol and evaluate how these processing parameters influence both the dispersion stability and the electrical conductivity of the resulting formulations. This stepwise approach enabled the separation of molecular structure effects from processing variables, allowing for a more comprehensive understanding of dispersion-performance relationships.

The influences of dispersion techniques on the characteristics of the prepared dispersions were investigated. FE-SEM imaging was employed to analyze the effectiveness of different dispersion methods and their morphological impacts on dispersed graphene nanoparticles.

Figure 4 depicts images from the jar milling method and magnetic stirring method, while the images attributed to ultrasonication are represented in Figure 1. The varying performance of SDBS surfactant across different dispersion methods stems from their distinct mechanisms:

1. **Jar Milling**: The rotational motion of milling pearls fragments graphene nanosheets through mechanical shear forces, leading to structural breakdown.
2. **Ultrasonication**: Intense ultrasonic waves create cavitation bubbles in the system. The subsequent bubble growth, coalescence, and violent collapse generate localized hotspots with sufficient energy to:
    - Break interparticle bonds
    - Disrupt some intramolecular bonds
    - Introduce structural defects in graphene lattices
    - Increase network imperfections
3. **Magnetic Stirring**: This gentler method applies lower shear stress, primarily separating graphene sheets without significant fragmentation, thereby better preserving their planar morphology [28-30].

As evident in the images, particle agglomeration occurs in all systems due to SDBS concentrations exceeding the critical micelle concentration (CMC).

Electrical resistivity measurements revealed that samples prepared via magnetic stirring exhibited significantly lower resistivity compared to both ultrasonicated and jar-milled samples, suggesting better preservation of graphene's conductive network.

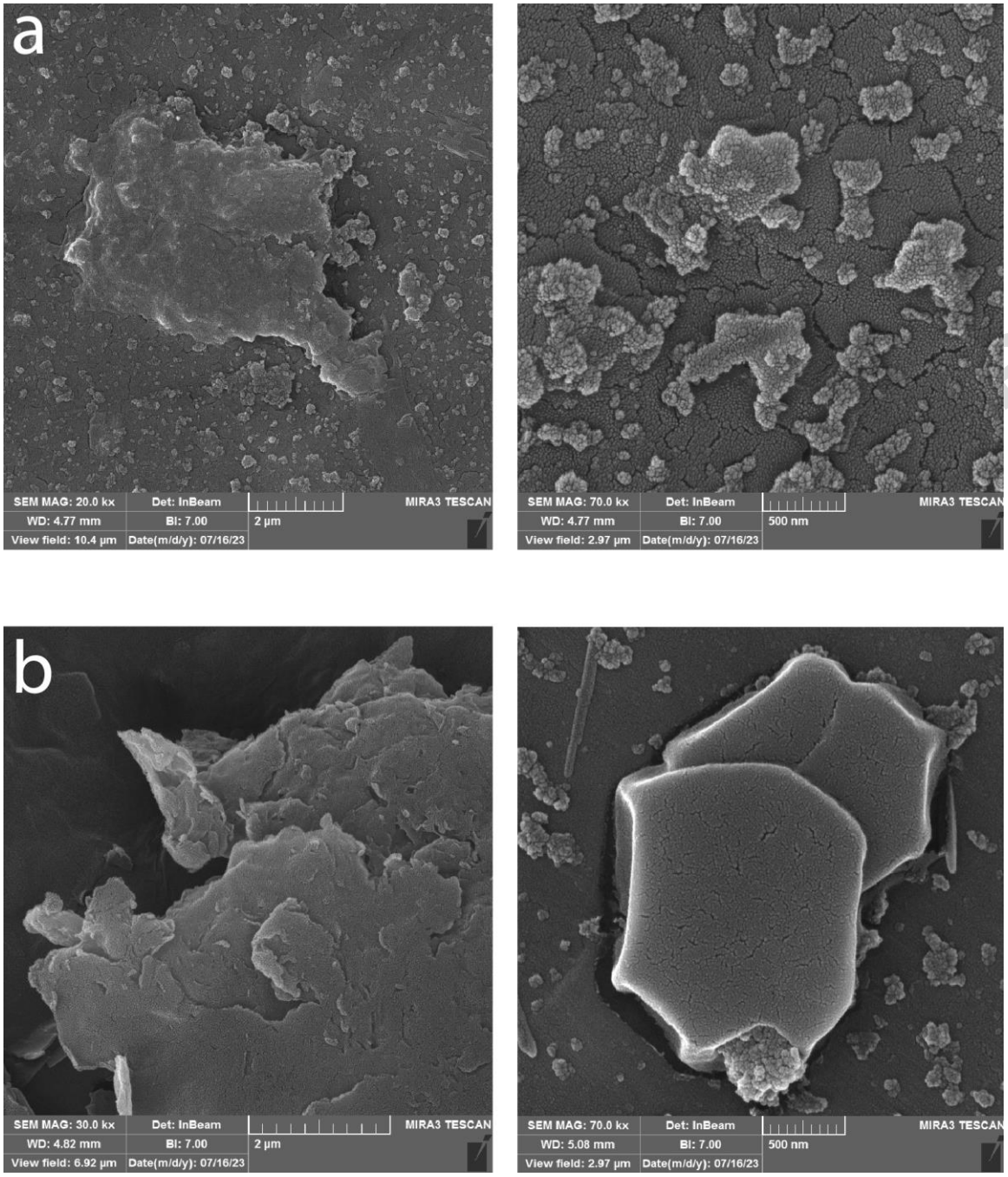


Figure 4: FE-SEM images showing morphology of (a) SDBS-0.25-JM and (b) SDBS-0.25-MS.

As shown in Table 4, the graphene dispersions prepared by ultrasonication and Jar milling exhibit higher electrical resistivity compared to those processed by magnetic stirring. Magnetic stirring yielded the lowest resistivity (24-32 MΩ) by preserving

graphene's structural integrity, unlike ultrasonication and jar milling, which introduced defects. This difference arises from greater sheet fragmentation during these more aggressive dispersion methods. The significantly reduced resistivity (and consequently higher conductivity) observed in the magnetically-stirred samples provide strong evidence for the superior effectiveness of this gentler dispersion approach. These findings reinforce the importance of balancing dispersion efficiency with structural preservation in conductive ink formulations. A key insight is that surfactants not only stabilize dispersions but also mediate the trade-off between exfoliation and damage to the conductive framework of graphene nanosheets.

Table 4: Electrical resistivity values of graphene dispersions prepared by different processing methods.

| Dispersion Method | Electrical resistivity (MΩ) |
|---|---|
| Jar mill | 38-64 |
| Ultrasonic | 53-89 |
| Magnetic stirrer | 24-32 |

### 3.3. The concentration of surfactant

Further investigations were conducted on three different concentrations of SDBS surfactant (0.1%, 0.25%, and 0.75%) using magnetic stirring dispersion followed by UV-vis spectroscopy. The image of the prepared samples is represented in Figure 5.

Figure 5: Photographic images of the graphene dispersions: (left) SDBS-0.75-MS, (middle) SDBS-0.25-MS, and (right) SDBS-0.10-MS.

Although graphene lacks distinct spectral peaks in the UV-Vis region due to its broad and featureless absorbance, this technique can still be useful for evaluating dispersion quality. In this study, the total absorbance at a fixed concentration was used as an indirect measure of dispersion quality. The rationale is that better-dispersed graphene nanosheets—those with smaller aggregate sizes and higher colloidal stability—exhibit higher light absorption owing to increased effective surface area and scattering. Thus, variations in the intensity of absorbance among samples were considered indicative of differences in the dispersion efficiency achieved by each surfactant. Figure 6 displays the corresponding absorption spectra for the three concentrations. The highest absorption intensity was observed for 0.1% SDBS, indicating both system stability and superior dispersion quality. Increasing the surfactant concentration (from 0.1% to 0.25% and 0.75%) resulted in decreased absorption, demonstrating graphene aggregation due to excessive micelle formation and partial sedimentation.

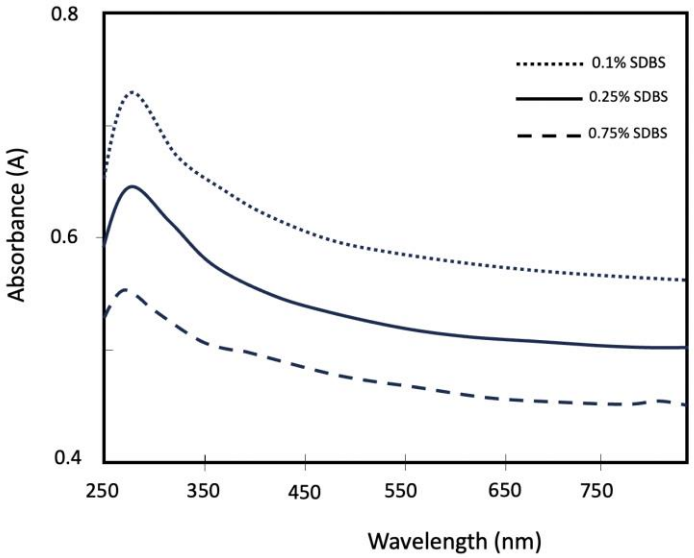


Figure 6: UV-Vis spectral analysis of graphene-based conductive ink at varying SDBS concentrations (0.1%, 0.25%, 0.75%).

As shown in Figure 6, the absorption peak at 284 nm confirms the preservation of π-conjugation in graphene, with SDBS showing the highest intensity due to optimal exfoliation. Reduction of SDBS surfactant concentration from 0.25% to 0.1% effectively improved the magnetic stirring method by:

• Minimizing particle aggregation

• Enhancing inter-sheet and edge-to-edge connectivity

• Reducing electrical resistivity by 15%

Figure 7 displays FE-SEM images demonstrating the optimized graphene dispersion achieved through reduced surfactant loading. Furthermore, the electrical resistivity of the 0.1% graphene sample decreased to the 4-18 MΩ range, confirming successful preservation of graphene's sheet-like structure [31]. The modified method resulted in:

1. Improved exfoliation efficiency
2. Established effective charge transport networks within the graphene architecture
3. Optimal micelle concentration without oversaturation

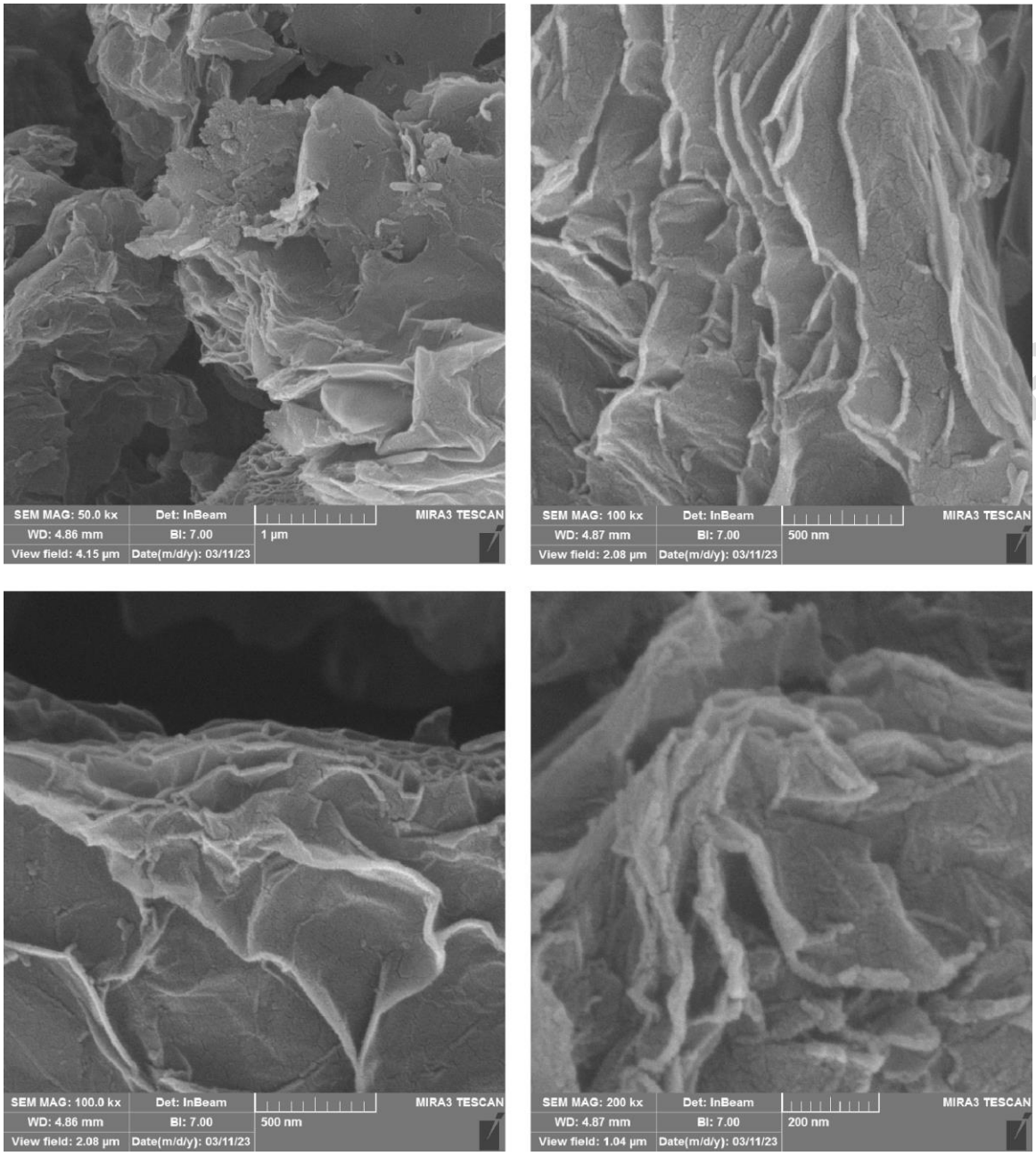


Figure 7: FE-SEM images showing morphological characterization of optimized graphene dispersions with 0.1% SDBS surfactant loading. Scale bar represents 1 µm.

## 4. Conclusion

This study demonstrated the pivotal role of surfactant type and concentration, as well as dispersion technique in determining the dispersion stability and electrical performance of graphene-based conductive inks. Key findings include:

**1-Surfactant Type**: Anionic surfactants, especially SDBS, exhibited superior dispersion stability and conductivity due to electrostatic repulsion and strong π-π interactions with graphene. Cationic (CTAB) and nonionic (Triton X-100) surfactants showed limited performance, attributed to micelle formation and steric hindrance.

**2-Concentration Optimization**: Surfactant concentrations near the CMC (e.g., 0.1% SDBS) achieved optimal dispersion, while higher concentrations (e.g., 0.75%) induced aggregation and increased resistivity.

**3-Dispersion Method**: Magnetic stirring preserved graphene's structural integrity and yielded the lowest resistivity (24-32 mΩ), outperforming ultrasonication and jar milling, which introduced defects.

**4-Characterization Techniques**: UV-Vis spectroscopy SEM analysis provided robust insights into dispersion quality and stabilization mechanisms.

These results underscore the importance of balancing surfactant chemistry, concentration, and processing methods to optimize ink performance. The study offers practical guidelines for formulating stable, high-conductivity water-based inks, addressing critical challenges in printed electronics. Future work could explore synergistic effects of surfactant blends and environmental stability of printed films.



## References

1. Kamyshny A, Magdassi S. Conductive nanomaterials for printed electronics. small. 2014; 10(17):3515-35. https://doi.org/10.1002/smll.201303000.

2. Khan S, Lorenzelli L, Dahiya RS. Technologies for printing sensors and electronics over large flexible substrates: a review. IEEE Sens J. 2015; 15(6):3164-85. https://doi.org/10.1109/JSEN.2014.2375203.

3. Tran TS, Dutta NK, Choudhury NR. Graphene inks for printed flexible electronics: Graphene dispersions, ink formulations, printing techniques and applications. Adv Colloid Interface Sci. 2018; 261:41-61. https://doi.org/10.1016/j.cis.2018.09.003.

4. Määttänen A, Ihalainen P, Pulkkinen P, Wang S, Tenhu H, Peltonen J. Inkjet-printed gold electrodes on paper: characterization and functionalization. ACS Appl Mater Interfac. 2012; 4(2):955-64. https://doi.org/10.1021/am201609w.

5. Magdassi S, World S. The chemistry of inkjet inks 2010. Available from: http://www.worldscientific.com/worldscibooks/10.1142/6869#t=toc.

6. Hajalifard Z, Mousazadeh M, Khademi S, Khademi N, Jamadi MH, Sillanpää M. The efficacious of AOP-based processes in concert with electrocoagulation in abatement of CECs from water/wastewater. npj Clean Water. 2023; 6(1):30. https://doi.org/10.1038/s41545-023-00239-9.

7. Jalili M, Naeini MMR, Ajili N. Optimizing dispersion in sublimation inkjet inks: unveiling the role of sodium naphthalene sulfonate formaldehyde condensate as a co-dispersant. J Coat Technol Res. 2025; 22(4):1557-72. https://doi.org/10.1007/s11998-024-01060-w.

8. Liang J, Tong K, Pei Q. A water-based silver-nanowire screen-print ink for the fabrication of stretchable conductors and wearable thin-film transistors. Adv Mater. 2016; 28(28):5986-96. https://doi.org/10.1002/adma.201600772.

9. Wang H, Qiao X, Chen J, Ding S. Preparation of silver nanoparticles by chemical reduction method. Colloids Surf Physicochem Eng Aspects. 2005; 256(2):111-5. https://doi.org/10.1016/j.colsurfa.2004.12.058.

10. Sirringhaus H, Shimoda T. Inkjet printing of functional materials. MRS Bull. 2003; 28(11):802-6. https://doi.org/10.1557/mrs2003.228.

11. Singh M, Haverinen HM, Dhagat P, Jabbour GE. Inkjet printing—process and its applications. Adv Mater. 2010; 22(6):673-85. https://doi.org/10.1002/adma.200901141.

12. Singh SK, Singh MK, Nayak MK, Kumari S, Shrivastava S, Grácio JJA, et al. Thrombus inducing property of atomically thin graphene oxide sheets. ACS Nano. 2011; 5(6):4987-96. https://doi.org/10.1021/nn201092p.

13. Dai G. Synthesis of carbon nanotubes by catalytic chemical vapor deposition. In: Saleh HM, El-Sheikh SMM, editors. Perspective of Carbon Nanotubes. Rijeka: IntechOpen; 2019.

14. Tadros TF. Adsorption of Surfactants and Polymeric Surfactants at the Solid/Liquid Interface. Applied Surfactants. 2005. p. 85-113.

15. Nayini MMR, Ranjbar Z. Carbon Nanotubes: Dispersion Challenge and How to Overcome It. In: Abraham J, Thomas S, Kalarikkal N, editors. Handbook of Carbon Nanotubes. Cham: Springer International Publishing; 2022. p. 341-92.

16. Španková M, Vávra I, Chromik Š, Gaži Š, Štrbík V, Kúš P, et al. Improvement of the superconducting properties of YBCO thin films upon annealing of $CeO_2/Al_2O_3$ substrate. Thin Solid Films. 2002; 416(1):254-9. https://doi.org/10.1016/S0040-6090(02)00629-6.

17. Lotya M, Hernandez Y, King PJ, Smith RJ, Nicolosi V, Karlsson LS, et al. Liquid phase production of graphene by exfoliation of graphite in surfactant/water solutions. J Amer Chem Soc. 2009; 131(10):3611-20. https://doi.org/10.1021/ja807449u.

18. Nazari B, Ranjbar Z, Moghaddam AR, Momen G, Ranjbar B. Dispersing graphene in aqueous media: Investigating the effect of different surfactants. Colloids Surf Physicochem Eng Aspects. 2019; 582:123870. https://doi.org/10.1016/j.colsurfa.2019.123870.

19. Mousazadeh M, Khademi N, Kabdaşlı I, Rezaei S, Hajalifard Z, Moosakhani Z, et al. Domestic greywater treatment using electrocoagulation-electrooxidation process: optimisation and experimental approaches. Sci Rep. 2023;13(1):15852. https://doi.org/10.1038/s41598-023-42831-6.

20. Zhang Q, Liu L, Pan C, Li D. Review of recent achievements in self-healing conductive materials and their applications. J Mater Sci. 2018; 53(1):27-46. https://doi.org/10.1007/s10853-017-1388-8.

21. Zhang X, Coleman AC, Katsonis N, Browne WR, van Wees BJ, Feringa BL. Dispersion of graphene in ethanol using a simple solvent exchange method. Chem Commun. 2010; 46(40):7539-41. https://doi.org/10.1039/C0CC02688C.

22. Hsiao A-E, Tsai S-Y, Hsu M-W, Chang S-J. Decoration of multi-walled carbon nanotubes by polymer wrapping and its application in MWCNT/polyethylene composites. Nanoscale Research Letters. 2012; 7(1):240. https://doi.org/10.1186/1556-276X-7-240.

23. Kango S, Kalia S, Celli A, Njuguna J, Habibi Y, Kumar R. Surface modification of inorganic nanoparticles for development of organic–inorganic nanocomposites—A

review. Prog Polym Sci. 2013; 38(8):1232-61. https://doi.org/10.1016/j.progpolymsci.2013.02.003.

24. Chaban VV, Fileti EE. Graphene exfoliation in ionic liquids: unified methodology. RSC Adv. 2015; 5(99):81229-34. https://doi.org/10.1039/C5RA16857K.

25. Vaisman L, Wagner HD, Marom G. The role of surfactants in dispersion of carbon nanotubes. Adv Colloid Interface Sci. 2006; 128-130:37-46. https://doi.org/10.1016/j.cis.2006.11.007.

26. Hashemi R, Weng GJ. A theoretical treatment of graphene nanocomposites with percolation threshold, tunneling-assisted conductivity and microcapacitor effect in AC and DC electrical settings. Carbon. 2016; 96:474-90. https://doi.org/10.1016/j.carbon.2015.09.103.

27. Lalire T, Longuet C, Taguet A. Electrical properties of graphene/multiphase polymer nanocomposites: A review. Carbon. 2024; 225:119055. https://doi.org/10.1016/j.carbon.2024.119055.

28. Wamsley M, Zou S, Zhang D. Advancing Evidence-Based Data Interpretation in UV–Vis and Fluorescence Analysis for Nanomaterials: An Analytical Chemistry Perspective. Anal Chem. 2023; 95(48):17426-37. https://doi.org/10.1021/acs.analchem.3c03490.

29. Dastyar P, Salehi MS, Firoozabadi B, Afshin H. Influences of polymer–surfactant interaction on the drop formation process: an experimental study. Langmuir. 2021; 37(3):1025-36. https://doi.org/10.1021/acs.langmuir.0c02487.

30. Jalili M, Mohammad Raei Naeini M, Bastani S, Ajili N. Optimizing the surfactant/polymeric dispersant combination in pigment-based aqueous inkjet inks. Prog Color Color Coat. 2025; 18(2):177-88. https://doi.org/10.30509/pccc.2024.167361.1316.

31. Wentzel D, Miller S, Sevostianov I. Dependence of the electrical conductivity of graphene reinforced epoxy resin on the stress level. Inter J Eng Sci. 2017; 120:63-70. https://doi.org/10.1016/j.ijengsci.2017.06.013.